Article

Cell Metabolism

A PDGFRα-Mediated Switch toward CD9^{high} Adipocyte Progenitors Controls Obesity-Induced Adipose Tissue Fibrosis

Graphical Abstract

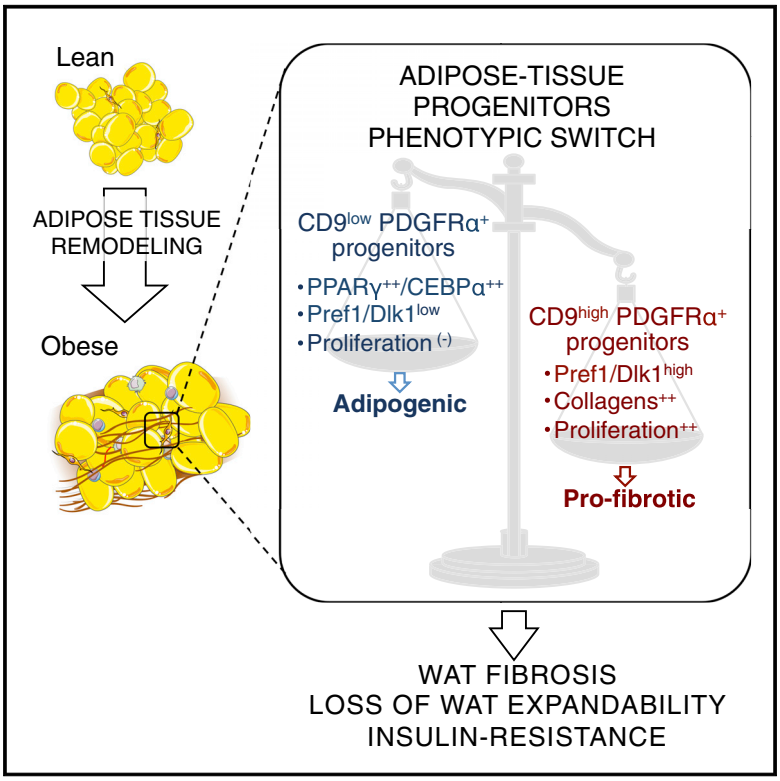

Highlights

- PDGFRα^{+} progenitors adopt a myofibroblastic phenotype in fibrotic adipose tissue
- CD9 expression delineates two subsets of adipose PDGFRα^{+} progenitors
- CD9^{high} progenitors are profibrogenic and drive adipose tissue fibrosis
- In obese subjects, increased CD9^{high} progenitors in fat are associated with diabetes

Authors

Geneviève Marcelin, Adaliene Ferreira, Yuejun Liu, ..., Jean-Christophe Bichet, Emmanuel L. Gautier, Karine Clément

Correspondence

genevieve_marcelin@yahoo.fr (G.M.), karine.clement2@gmail.com (K.C.)

In Brief

In obese subjects, white adipose tissue (WAT) fibrosis represents a maladaptive mechanism contributing to the loss of metabolic fitness and obesity-associated comorbidities. Marcelin et al. demonstrate that elevated PDGFRα^{+} progenitor subsets with high CD9 expression promote WAT fibrosis and are associated with metabolic deteriorations in mice and humans.

Accession Numbers

GSE84823

Marcelin et al., 2017, Cell Metabolism *25*, 673–685
March 7, 2017
http://dx.doi.org/10.1016/j.cmet.2017.01.010

Cell Metabolism
Article

A PDGFRα-Mediated Switch toward CD9^{high} Adipocyte Progenitors Controls Obesity-Induced Adipose Tissue Fibrosis

Geneviève Marcelin,[1,2,4,*] Adaliene Ferreira,[1,2,5] Yuejun Liu,[1,2,3,4] Michael Atlan,[8] Judith Aron-Wisnewsky,[1,2,3,4] Véronique Pelloux,[1,2,4] Yair Botbol,[6] Marc Ambrosini,[1,2,4] Magali Fradet,[1] Christine Rouault,[1,2,4] Corneliu Hénégar,[7] Jean-Sébastien Hulot,[1,2,4] Christine Poitou,[1,2,3,4] Adriana Torcivia,[3] Raphael Nail-Barthelemy,[8] Jean-Christophe Bichet,[9] Emmanuel L. Gautier,[1,2,4] and Karine Clément[1,2,3,4,10,*]

[1]Institute of Cardiometabolism and Nutrition, ICAN, Pitié-Salpêtrière Hospital, F-75013 Paris, France
[2]INSERM, UMRS 1166 (teams 2, 4, and 6 NutriOmics), F-75013 Paris, France
[3]Assistance Publique Hopitaux de Paris, AP-HP, Pitié-Salpêtrière Hospital, Nutrition and Endocrinology Department and Hepato-biliary and Digestive Surgery Department, F-75013 Paris, France
[4]Sorbonne Universités, UPMC Univ Paris 06, UMRS 1166, F-75013 Paris, France
[5]Immunometabolism, Department of Nutrition, Nursing School, Universidade Federal de Minas Gerais, Belo Horizonte 31270-901, Brazil
[6]Department of Pathology, Albert Einstein College of Medicine, Bronx, NY 10461, USA
[7]HudsonAlpha Institute for Biotechnology, 601 Genome Way, Huntsville, AL 35806, USA
[8]Assistance Publique Hôpitaux de Paris, Aesthetic Plastic Reconstructive Unit, Tenon Hospital, Sorbonne Universités, UPMC Univ Paris 06, UMR_S 1166, 75020 Paris, France
[9]Assistance Publique Hôpitaux de Paris, Plastic Surgery and Mammary Cancer Department, Pitié-Salpêtrière Hospital, F-75013 Paris, France
[10]Lead Contact
*Correspondence: genevieve_marcelin@yahoo.fr (G.M.), karine.clement2@gmail.com (K.C.)
http://dx.doi.org/10.1016/j.cmet.2017.01.010

SUMMARY

Obesity-induced white adipose tissue (WAT) fibrosis is believed to accelerate WAT dysfunction. However, the cellular origin of WAT fibrosis remains unclear. Here, we show that adipocyte platelet-derived growth factor receptor-α-positive (PDGFRα^{+}) progenitors adopt a fibrogenic phenotype in obese mice prone to visceral WAT fibrosis. More specifically, a subset of PDGFRα^{+} cells with high CD9 expression (CD9^{high}) originates pro-fibrotic cells whereas their CD9^{low} counterparts, committed to adipogenesis, are almost completely lost in the fibrotic WAT. PDGFRα pathway activation promotes a phenotypic shift toward PDGFRα^{+}CD9^{high} fibrogenic cells, driving pathological remodeling and altering WAT function in obesity. These findings translated to human obesity as the frequency of CD9^{high} progenitors in omental WAT (oWAT) correlates with oWAT fibrosis level, insulin-resistance severity, and type 2 diabetes. Collectively, our data demonstrate that in addition to representing a WAT adipogenic niche, different PDGFRα^{+} cell subsets modulate obesity-induced WAT fibrogenesis and are associated with loss of metabolic fitness.

INTRODUCTION

Obesity is a clinically and biologically complex disease where appetite and energy metabolism are dysregulated. In obese individuals, both visceral and subcutaneous white adipose tissue (WAT) depots expand to buffer the nutrient excess (Sun et al., 2011). Patients with higher visceral fat mass are at a higher risk of developing severe complications such as type 2 diabetes (T2D) and cardiovascular and liver diseases, whereas patients with predominant subcutaneous fat storage have a reduced risk of metabolic diseases (Kissebah and Krakower, 1994; Wajchenberg, 2000; Ibrahim, 2010).

In response to chronic nutrient overload, WAT depots undergo continual remodeling, becoming pathological in the obese state. It is now clear that pro-inflammatory cell accumulation favors local WAT injury and dysfunction (Dalmas et al., 2014), thus perturbing systemic homeostasis (Hotamisligil et al., 1993; Weisberg et al., 2003; Osborn and Olefsky, 2012). More recently, excess levels of extracellular matrix (ECM) and fibrosis were described in WAT depots from obese individuals (Henegar et al., 2008; Divoux et al., 2010) and studies have linked ECM deposition to modified WAT metabolic and endocrine function (Pellegrinelli et al., 2014a; Sun et al., 2013; Pasarica et al., 2009; Spencer et al., 2010; Guglielmi et al., 2015). In obese mice, targeting ECM remodeling was shown to improve glucose tolerance and insulin sensitivity (Khan et al., 2009; Halberg et al., 2009). Therefore, WAT fibrosis could represent a maladaptive mechanism contributing to obesity-related metabolic complications. Thereby, there is an urgent need to better understand the mechanisms underlying fibrosis development in obesity and its related comorbidities. It is generally accepted that fibrosis is mediated by tissue-resident cells, which, when activated, locally transform into myofibroblasts (Wynn, 2008). In injured muscle or in muscular dystrophies, bipotent fibro/adipogenic progenitors have been shown to give rise to adipocytes and collagen-producing cells that compromised muscle function. These progenitors were identified with markers similar to those found on adipogenic progenitors isolated from WAT (Joe et al., 2010; Uezumi et al., 2010, 2011). However, it is not known whether

mechanisms underlying both fibrosis and ectopic fat formation in injured muscle differ from those driving homeostatic adipogenesis and pathological fibrosis in WAT. Indeed, pro-fibrotic cells have not yet been accurately identified in obese WAT.

Thus, we set out to define those cells significantly producing ECM in murine obese WAT. Here, we identified that mouse adipocyte progenitors, defined as platelet-derived growth factor receptor-α-positive cells (PDGFRα$^+$) (Rodeheffer et al., 2008), adopted a myofibrobastic phenotype that promotes ECM deposition and WAT fibrosis. Combining experiments in mouse models and human conditions, we report here that PDGFRα$^+$ CD9^{high} cells originate pro-fibrotic cells, while their CD9^{low} counterparts harbored pro-adipogenic potential. Activation of the pro-fibrotic PDGFRα pathway (Olson and Soriano, 2009) promotes a phenotypic switch toward CD9^{high}PDGFRα$^+$ pro-fibrotic cells, thus driving morphological and functional alterations in obese WAT. Most importantly, we translated these findings to human obesity, as we demonstrated that the frequency of PDGFRα$^+$CD9^{high} in omental WAT (oWAT) correlated not only to oWAT fibrosis level but also to the severity of insulin resistance and T2D. Collectively, our data show that different PDGFRα$^+$ cell subsets are able to modulate obesity-induced WAT fibrogenesis and major obesity-related metabolic alterations.

RESULTS

Obesity-Induced Fibrosis in Epididymal Fat Pad of C3H Mice Limits Fat Expansion and Is Associated with Insulin Resistance

To investigate the cellular and molecular determinants of obesity-induced WAT fibrosis, we compared two mouse strains: C57BL6/J (B6) strain and C3H/HeOuj (C3H) mice reported to display differential susceptibility to WAT fibrosis (Vila et al., 2014). We aimed to compare the fibrosis level in mice with similar degrees of obesity. The C3H males only required 2 months of high-fat diet (HFD) feeding to reach an equivalent body weight of B6 males HFD fed for 3 months (Figure 1A). However, B6 males exhibited a slightly increased body fat mass as compared to C3H animals (Figure 1B). Quantifying hydroxyproline in inguinal (IngWAT) and epididymal (EpiWAT) fat pad depots revealed major differences. In response to HFD, collagen accumulation was evident in the EpiWAT of C3H animals, but not in that of B6 mice, nor in the IngWAT of both strains (Figures 1C, 1D, and S1A, available online). HFD feeding upregulated the mRNA expression of many fibrosis and cross-linking enzyme genes in the EpiWAT of both strains (*Col1a1*, *Col3a1*, *Fn1*, *Tnc*, *Tgfb1*, and *Loxl2*), but their level of expression was always higher in the obese C3H animals (Figure 1E). This observation confirms that WAT fibrosis is more advanced in EpiWAT of C3H, as compared to B6 animals with similar body weight.

In response to HFD feeding (2 months for C3H and 3 months for B6), EpiWAT mass significantly increased in B6, but not in C3H animals (Figure 1F). More specifically, in growing HFD-fed C3H mice (Figure S1B), EpiWAT mass significantly increased during the first 3 weeks of HFD feeding, which then plateaued (Figure S1C). Concomitantly, EpiWAT hydroxyproline content started to increase (Figure S1D). In contrast, IngWAT increased similarly in both C3H and B6 strains (Figure 1G). In addition, IngWAT mass increased gradually in HFD-fed C3H mice (Figure S1E) without more collagen deposition after starting HFD feeding (Figure S1F). We further observed that EpiWAT fibrosis was associated with decreased mRNA expression of *Leptin* and *Adiponectin* genes in EpiWAT of obese C3H animals compared to B6 mice (Figure 1H). By contrast, the non-fibrotic IngWAT of C3H displayed upregulated *Leptin* mRNA and unchanged *Adiponectin* mRNA expression in response to HFD feeding (Figure S1G), similar to B6 EpiWAT. This finding suggests that the decreased expression of *Leptin* and *Adiponectin* in the fibrotic EpiWAT of C3H is a witness of tissue loss of function. Insulin sensitivity was markedly lower in EpiWAT of C3H mice as measured by AKT Ser473 phosphorylation (^{pS473}AKT) in response to insulin (Figure 1I). In contrast, the insulin-dependent ^{pS473}AKT response was similar in the non-fibrotic IngWAT of both mouse strains (Figure 1J).

Overall, C3H animals are characterized by an increased propensity for WAT fibrosis and we propose that fibrosis most likely limits early EpiWAT expansion, which is associated with functional WAT alterations. This model thus appeared appropriate to further explore the cellular effectors of WAT fibrosis.

PDGFRα$^+$ Progenitors Are Cellular Effectors of Obesity-Induced EpiWAT Fibrosis

In many tissues, fibrosis is mediated by cell transformation toward a so-called myofibroblast phenotype, with upregulated αSMA expression and ECM production (Wynn, 2008).

Following collagenase digestion of fibrotic EpiWAT, from obese C3H mice, we harvested floating adipocytes and sorted endothelial cells (CD45$^-$ CD31$^+$), macrophages (CD45$^+$ F4/80$^+$ CD11b$^+$), and adipose progenitors (Rodeheffer et al., 2008), defined as PDGFRα$^+$, Gp38$^+$, CD45$^-$, and CD31$^-$ (Figures 2A, S2, and S3). We examined the mRNA expression of fibrosis markers and found that ECM components (*Col1a1*, *Col3a1*, *Col6a1*, and *Fn1*) and cross-linking enzymes (*Lox* and *Loxl2*) were approximately 100- to 200-fold greater in PDGFRα$^+$ progenitors as compared to other cell types (Figure 2B).

HFD feeding led to increased PDGFRα$^+$cell number per EpiWAT pad from B6 and C3H mice (Figure 2C). However, cell density (i.e., cell count per gram of fat) increased only in C3H (Figure 2D), likely due to constrained EpiWAT growth as described above. HFD feeding significantly increased the proliferation rate determined via Ki-67 expression (Cuylen et al., 2016) in both strains, but with greater increase in C3H EpiWAT than in B6 EpiWAT (Figures 2E and 2F).

We further characterized PDGFRα$^+$ progenitors isolated from EpiWAT of lean and obese C3H mice by analyzing their gene expression profile (Figure 2G). *Acta2* mRNA level, encoding for the αSMA myofibroblast marker, was induced more than 4-fold in progenitors isolated from obese C3H compared to lean C3H mice. Expression of mRNA transcripts encoding pro-fibrotic cytokines (*Ctgf* and *Inha*) and ECM proteins (*Col1a1*, *Fn1*, and *Tnc*) was also upregulated as well as pro-inflammatory mediators *Il6*, *Ccl2*, *Ccl7*, and *Cxcl10* (Figure 2G). Overall, we showed that increased PDGFRα$^+$ density driven by elevated proliferation rates highly contributed to fibrotic gene expression in the EpiWAT of HFD-fed C3H mice.

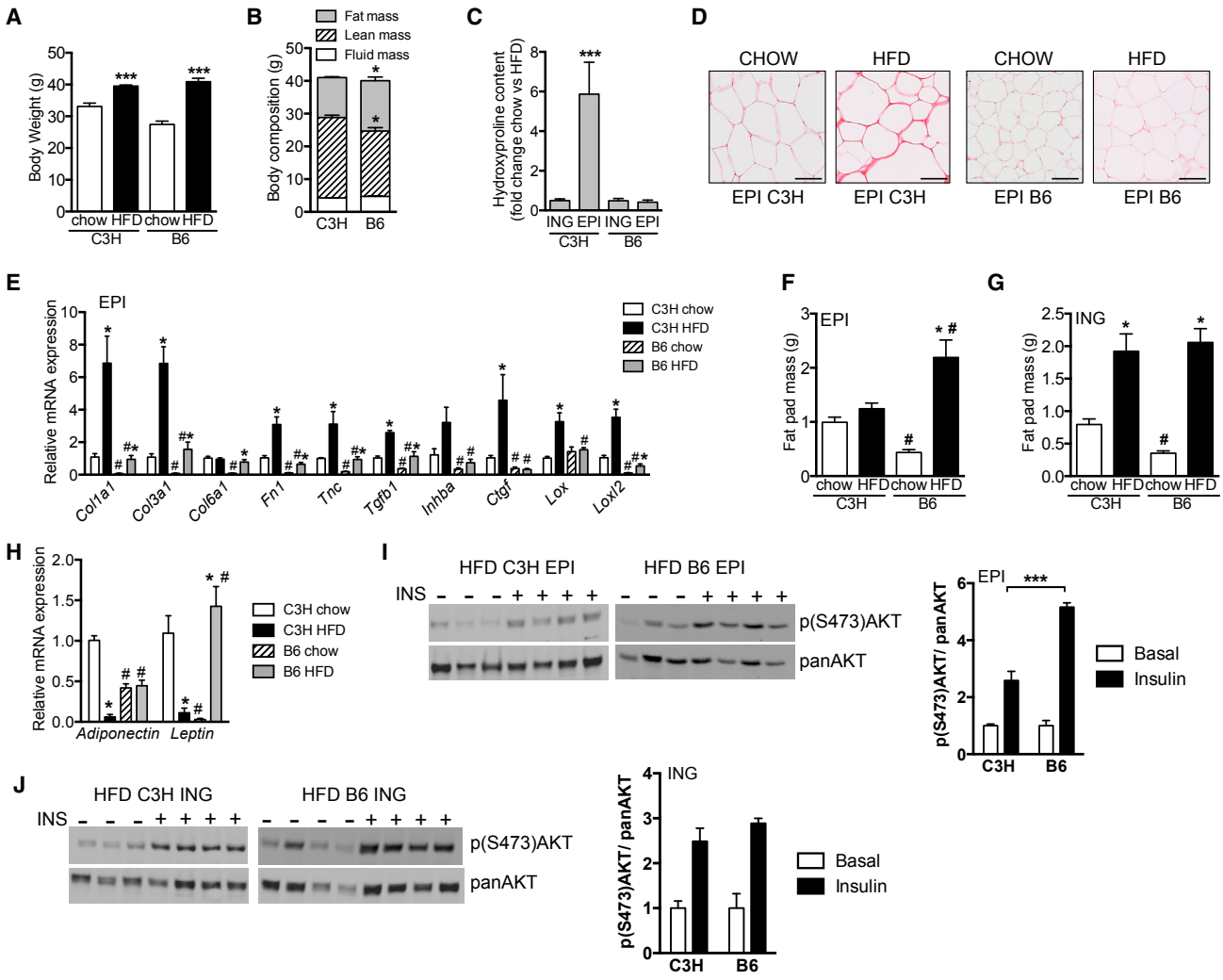

Figure 1. Comparison between Body Weight-Matched C3H and B6 Mice

Chow and HFD feeding started in 6-week-old animals for 2 or 3 months in C3H or B6 mice, respectively.

(A) Body weight measured in chow- and HFD-fed C3H and B6 mice (n = 5–10).

(B) Body composition in HFD-fed C3H and B6 mice (n = 5–10).

(C) Hydroxyproline content in WAT of C3H and B6 animals. Data are presented as fold increase between lean (chow) and obese (HFD) conditions in EpiWAT and IngWAT (n = 4–5).

(D) Representative red picrosirius-stained paraffin section of EpiWAT from chow- and HFD-fed C3H and B6 mice; scale bar, 100 μm.

(E) mRNA expression of fibrosis markers in the EpiWAT of chow- and HFD-fed B6 and C3H mice (n = 5–7). Data are normalized against C3H chow condition.

(F and G) Epididymal (F) and inguinal (G) fat pad mass of lean and HFD-fed C3H and B6 animals (n = 4–5).

(H) Relative mRNA expression of *Adiponectin* and *Leptin* in EpiWAT of lean and obese animals (n = 5–7).

(I and J) Ser473 phosphorylation of AKT (p(S473)AKT) and pan AKT expression in (I) epidymal and (J) inguinal fat of HFD-fed C3H and B6 males injected with insulin (+INS) or not (−INS).Quantification of p(S473)AKT normalized against panAKT relative to basal condition is presented (n = 3–4). *p < 0.05, **p < 0.005, ***p < 0.0005 between chow and HFD conditions; #p < 0.05 between lean or obese C3H and B6 groups.

Data are expressed as mean ± SEM.

PDGFRα+ Progenitors Display Pro-fibrotic Features in Human Obese WAT

In concurrence with mouse findings, SVF cells, but not isolated adipocytes, expressed PDGFRα in obese human oWAT (Figure 3A), and WAT progenitors (Estève et al., 2015) were identified as CD31− CD45− CD34+ CD44+ PDGFRα+ cells (Figure 3B). The pro-fibrotic cytokine TGFβ is induced in both mouse and human WAT during obesity and may contribute to WAT fibrosis (Chun et al., 2006; Vila et al., 2014). To assess whether human PDGFRα+ progenitors could acquire a pro-fibrotic phenotype in response to a pro-fibrotic stimulus, we treated these cells with TGFβ. We found that PDGFRα+ progenitors isolated from lean subcutaneous WAT (scWAT) demonstrated robust increased mRNA expression of a number of fibrosis markers (Figure 3C), in addition to the myofibroblast marker αSMA (Figure 3D). Immunofluorescence analysis indicated that PDGFRα+

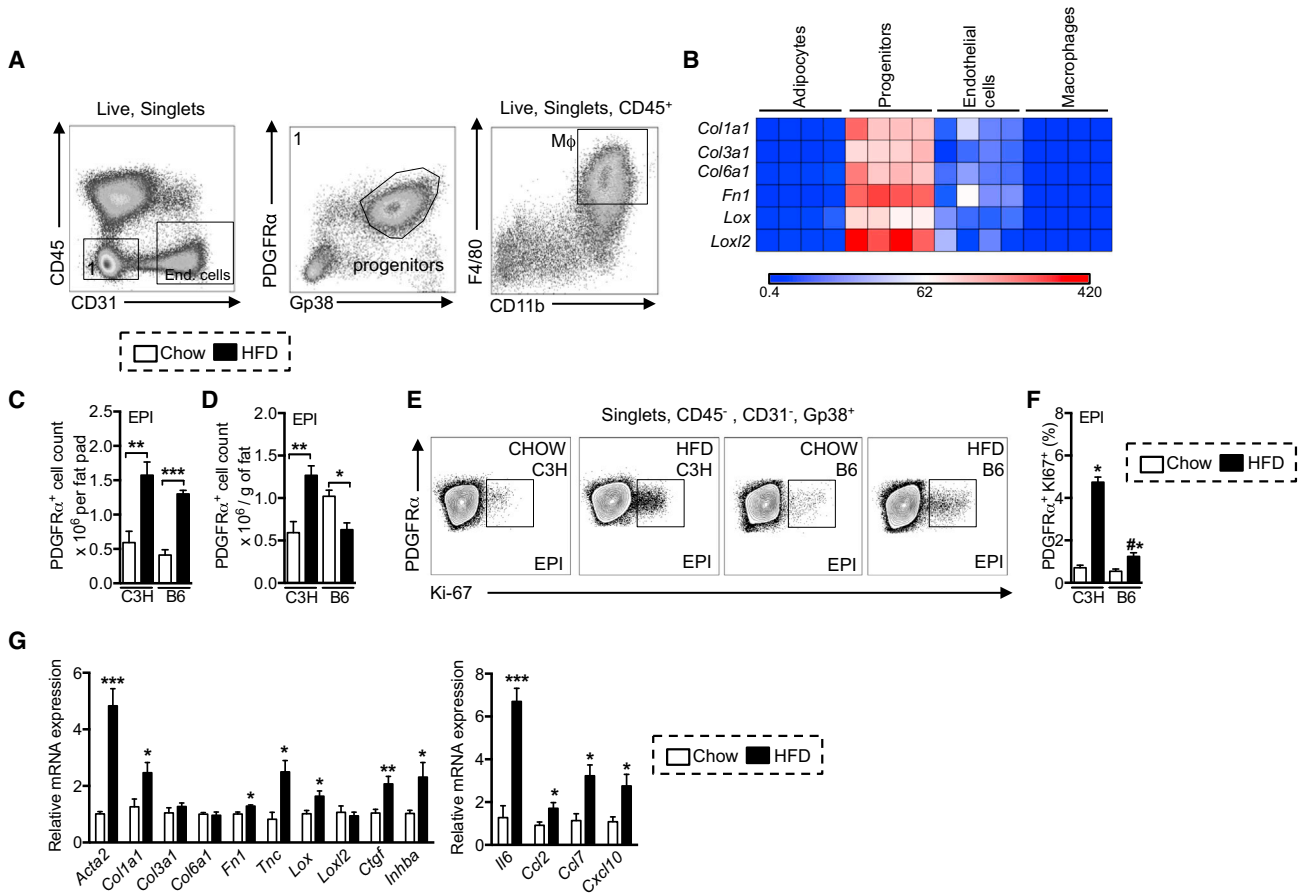

Figure 2. PDGFRα⁺ Progenitors in Obesity-Induced WAT Fibrosis

(A) FACS plot showing the gating strategy for macrophages, endothelials cells, and adipose progenitor cell sorting from EpiWAT of C3H mice.

(B) Heatmap depicting fibrosis marker expression in adipocytes, progenitors, endothelial cells, and macrophages obtained from EpiWAT of obese C3H mice (n = 4).

(C and D) Progenitor cell count (C) per fat pad or (D) per gram of fat in EpiWAT of chow and HFD C3H and B6 mice. Quantification was performed with flow cytometry (n = 4–5).

(E) Representative flow cytogram of Ki-67 expression on CD45⁻, CD31⁻, Gp38⁺, and PDGFRα⁺ cells isolated from EpiWAT SVF.

(F) Percentage of PDGFRα⁺ Ki-67⁺ in EpiWAT of chow and HFD C3H and B6 mice (n = 4–5).

(G) Gene expression analysis performed in progenitors (CD45⁻ CD31⁻ PDGFRα⁺ Gp38⁺) sorted with flow cytometry from EpiWAT of lean and obese C3H animals (n = 4). *p < 0.05, **p < 0.005, ***p < 0.0005 between chow and HFD conditions. C3H and B6 obese mice were fed on HFD for 2 and 3 months, respectively. Data are expressed as mean ± SEM.

cells freshly isolated from oWAT of obese individuals expressed ECM proteins such as fibronectin, αSMA, and the fibrillar collagen I (Figure 3E). Furthermore, confocal imaging of oWAT from obese subjects showed that some PDGFRα⁺ cells co-expressed αSMA (Figure 3F), suggesting PDGFRα⁺ cells could also differentiate into myofibroblasts in vivo.

CD9 Expression Reveals Heterogeneity among WAT Progenitors Associated with Different Pro-fibrotic Potential

Our next objective was to identify markers that could differentiate between progenitor populations in relation to WAT fibrosis. Revisiting previous microarray analysis (Henegar et al., 2008) performed in human WAT led us to highlight CD9, whose expression was tightly co-regulated with many ECM or fibrosis genes (Table 1). CD9 has been implicated in a number of cellular processes including adhesion, migration, or signal transduction (Kim et al., 2007). A functional role for CD9 has been suggested, as CD9 knockdown with small interfering RNA (siRNA) in human AT progenitor cells in vitro reduced proliferation and increased the expression of pro-adipogenic markers (Holley et al., 2015).

Using flow cytometry, we identified $CD9^{high}$ and $CD9^{low}$ PDGFRα⁺ subsets in the EpiWAT of lean mice (Figure 4A). We demonstrated that $CD9^{high}$ progenitors displayed higher proliferation rates than $CD9^{low}$ precursor subsets in lean mice via Ki-67 expression (Figure 4C). Previous work identified a small fraction of PDGFRα⁺ progenitors expressing CD24⁺ that actively proliferate to enlarge the pool of post-mitotic PDGFRα⁺CD24⁻ able to differentiate into mature adipocyte (Rodeheffer et al., 2008). In the EpiWAT of lean C3H mice, CD24 was expressed in both

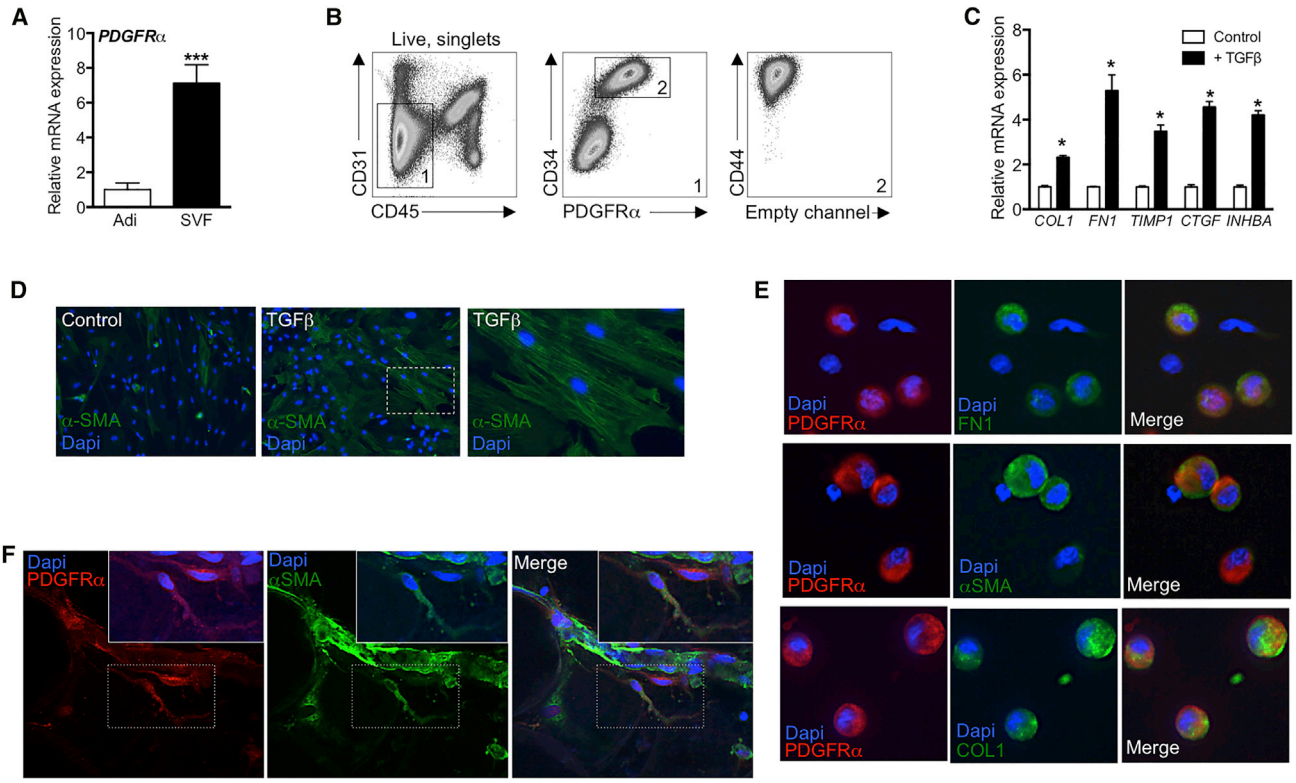

Figure 3. PDGFRα⁺ Progenitors in Human WAT

(A) *PDGFRα* mRNA expression in adipocytes and SVF isolated from obese oWAT (n = 5).

(B) FACS plots illustrating the gating strategy used for identification of progenitors in SVF in human WAT.

(C) In serum-deprived condition, $CD45^{-}CD31^{-}CD34^{+}$ immunoselected progenitors from scWAT of lean subject were treated for 5 days with 5 ng/mL TGFβ and mRNA expression analysis was performed (n = 3).

(D) Immunofluorescent (IF) detection of α-SMA (green) and DAPI (blue) in WAT progenitors treated or not treated with TGFβ.

(E) IF detection of PDGFRα (red), fibronectin (FN1, green), collagen 1 (COL1, green), αSMA (green), and DAPI (blue) in freshly isolated SVF cells from obese human oWAT.

(F) Whole-mount confocal imaging of PDGFRα (red), αSMA (green), and DAPI (blue) in obese human oWAT. *$p < 0.05$, ***$p < 0.0005$.

Data are expressed as mean ± SEM.

PDGFRα⁺ $CD9^{high}$ and PDGFRα⁺ $CD9^{low}$ cell subsets; thus, this marker did not discriminate these two cell subsets (Figure S4A).

Under obese conditions, the PDGFRα⁺ $CD9^{low}$ population was severely diminished in fibrotic and atrophic EpiWAT of C3H mice (Figures 4A and 4B) as compared to lean animals. Similarly, in the fibrotic peri-ovarian WAT (OvaWAT) of HFD-fed C3H females, we observed an increased frequency of PDGFRα⁺$CD9^{high}$ progenitors over the PDGFRα⁺ $CD9^{low}$ cells (Figure S4B), indicating absence of gender specificity concerning WAT fibrogenesis in C3H strain. In the less-fibrotic EpiWAT of obese B6 mice, we also observed increases in $CD9^{high}$ over $CD9^{low}$ progenitors, but to a significantly lesser extent than in C3H animals (Figures 4A and 4B). In the IngWAT of lean C3H mice, CD9 expression also defines two progenitor populations. In response to high-fat feeding, the IngWAT did not become fibrotic (Figures 1C and S1A) and the ratio of $CD9^{high}$ versus $CD9^{low}$ progenitors remained unchanged between lean and obese conditions (77.2% ± 1.5% and 79.6% ± 1.3% of PDGFRα⁺$CD9^{high}$ in the IngWAT from chow- and HFD-fed C3H mice, respectively).

Next, using whole-mouse genome arrays, we compared the transcriptional profiles of $CD9^{low}$ and $CD9^{high}$ progenitors isolated from EpiWAT of lean C3H mice by cell sorting. Gene set enrichment analysis (GSEA) clearly discriminated the two cell subtypes (Figures 4D and S4C). Genes involved in ECM organization and TGFβ signaling were enriched in $CD9^{high}$ progenitors, whereas genes relating to adipogenesis as well as lipid metabolism were enriched in their $CD9^{low}$ counterparts (Figures 4D and S4C). Expression analysis on cells sorted in an independent experiment confirmed increased expression of ECM-related genes in $CD9^{high}$ relative to $CD9^{low}$ progenitors (Figure 4E). In these $CD9^{high}$ cells, increased ECM gene expression was concomitant with reduced expression of pro-adipogenic transcription factors *Pparγ* and *Cebpα*, and high expression of the anti-adipogenic factor *Dlk1* (also known as *Pref1*) (Figure 4F).

Together, these results suggest that the two populations are functionally different; PDGFRα⁺ $CD9^{high}$ are driven toward ECM production, whereas PDGFRα⁺ $CD9^{low}$ cells are committed to adipogenesis. An adipocyte differentiation assay further supported this premise as PDGFRα⁺ $CD9^{low}$ cells were more prone to differentiate into adipocytes than their PDGFRα⁺ $CD9^{high}$ counterparts (Figure 4G). Moreover, WAT progenitors from

Table 1. GSEA of Gene Significantly Correlated with CD9 Expression

Gene Set Name	Description	FDR q value	Genes
Reactome_Immune System	genes involved in immune system	9.89E−09	CTSS, CTSB, CTSC, C1QC, ITGAV, VCAM1, ITGB5, PDPK1, ITGB2, PDIA3, LNPEP, PSMD14, LYN, HLA-DQA1, MAP3K8, RICTOR, PTPRC, KLC1, LCP2, FCGR3A, UBE2Z, CSF2RB, NUP107, IL1R1, IRS2, KPNA2, and CFH
NABA_Matrisome	genes encoding ECM and ECM-associated proteins	9.89E−09	CTSS, CTSB, CTSC, C1QC, COL4A1, SPP1, LAMB1, SERPINH1, ADAM12, CD109, LOX, ADAM9, FGF1, CXCL1, CCL18, IL15, SFRP4, ISM1, EGFL6, ANXA1, ANXA5, CLEC4A, COL5A2, COL12A1, LUM, CTHRC1, SRPX2, and SVEP1
Reactome_Adaptive Immune System	genes involved in adaptive immune system	3.07E−08	CTSS, CTSB, CTSC, C1QC, ITGAV, VCAM1, ITGB5, PDPK1, ITGB2, PDIA3, LNPEP, PSMD14, LYN, HLA-DQA1, MAP3K8, RICTOR, PTPRC, KLC1, LCP2, FCGR3A, and UBE2Z
Reactome_Integrin Cell Surface Interactions	genes involved in Integrin cell-surface interactions	6.70E−06	ITGAV, VCAM1, ITGB5, PDPK1, ITGB2, COL4A1, SPP1, and LAMB1
KEGG_Lysosome	lysosome	1.05E−05	CTSS, CTSB, CTSC, AP3S1, GLB1, ASAH1, AGA, LIPA, and LAPTM4B

Genes are with Pearson correlation coefficient $\geq$ 0.5 and $p < 0.005$ in subcutaneous adipose tissue from obese subjects (Henegar et al., 2008). Top five canonical pathways found significantly enriched using GSEA software are shown.

obese C3H EpiWAT (all CD9^{high}) (Figure 4A) did not differentiate into adipocytes (Figure 4H).

We then examined the impact of HFD feeding on progenitor phenotype, particularly focusing on CD9^{low} progenitors after limited (3 week) HFD exposure (Figure 4I). Even at this early stage, CD9^{low} progenitors began to demonstrate dysfunctionality as they downregulated *Pparγ* and *Cebpα* mRNA expression, and increased *Dlk1* (Figure 4J). Similar to CD9^{high} progenitors, CD9^{low} cells started to induce fibrosis marker gene expression (*Col1a1*, *Col3a1*, *Fn1*, *Lox*, and *Ctgf*) as well as the pro-inflammatory gene *Il6* (Figure 4J). Thus, CD9^{low} progenitors, committed to adipogenesis in lean EpiWAT, also responded to short-term HFD and rapidly lost their adipogenic orientation in switching toward a pro-fibrotic phenotype. This phenotypic switch preceded their complete loss upon longer periods of HFD feeding.

Increased PDGF-PDGFRα Signaling Components Impact WAT Homeostasis

In addition to being a marker of adipocyte progenitors, PDGFRα is also a well-described mediator of tissue fibrosis (Olson and Soriano, 2009). However, its role in obesity and WAT dysfunction has never previously been investigated. By exploring selective ligands of PDGFRα, we found that *Pdgfa* and *Pdgfc* expression was higher in EpiWAT from C3H animals as compared to B6 mice, both under chow and HFD conditions (Figure 5A). We thus hypothesized that increased signaling through PDGFRα could partly explain the susceptibility to fibrosis in C3H EpiWAT. We also detected higher *PDGFA* mRNA expression (Figure 5B) as well as PDGFAA secretion (Figure 5C) in scWAT of human obese as compared to lean samples. *PDGFC* mRNA expression was also higher in oWAT of obese subjects with T2D (Figure 5D). Moreover, incubation of immunoselected WAT progenitors with recombinant PDGFAA stimulated the production of the fibrillar collagen I (Figure 5E).

As PDGFRα ligands were upregulated (Figures 5A–5D) in WAT during obesity, we further analyzed whether cell-autonomous activation of a pro-fibrotic program promoted a phenotypic switch of the PDGFRα^{+} progenitors toward CD9^{high} cells. We used a mouse model bearing a Cre/lox-inducible PDGFRα with increased tyrosine kinase activity due to the D842V mutation (*PDGFRα$^{+/D842V}$* mice) (Olson and Soriano, 2009). Here, to probe the consequences of PDGFRα activation in PDGFRα^{+} progenitors on WAT function, we crossed *PDGFRα^{D842V}* animals with PDGFRα-CreERT2 mice that specifically express the Cre recombinase in PDGFRα-expressing cells upon tamoxifen treatment and fed these mice with HFD (Lee et al., 2012; Rivers et al., 2008).

We assessed the CRE recombination in sorted PDGFRα^{+} progenitors from PDGFRα-CreERT2 × *PDGFRα$^{+/D842V}$* mice (called *PdgfraKI* mutants) or their controls, using qPCR as reported (Olson and Soriano, 2009), and significant recombination was observed in OvaWAT of *PdgfraKI* mice (Figure S5A). We also quantified the percentage of PDGFRα^{+} displaying Cre-mediated recombination by using the fluorescent reporter model mT/mG and found about 10% of PDGFRα^{+} cells were labeled in the OvaWAT (Figure S5B).

At 2 months old, tamoxifen-treated control and *PdgfraKI* mutants were placed on an HFD in order to examine OvaWAT in the *PdgfraKI* mice in the context of HFD-induced obesity (Figure 5F). Early after Cre induction (15 days after the last tamoxifen administration), we did not observe any difference in body weight (Figure S5C) and fat mass (Figure S5D) or OvaWAT mass (Figure S5E) and morphology (Figure S5F) between control and *PdgfraKI* animals. After 2 months of HFD feeding, mutant mice displayed lower fat mass (Figure 5G) and the OvaWAT depot was smaller (Figure 5H) with decreased adipocyte size (Figure 5I). Sustained PDGFRα activation in a fraction of PDGFRα^{+} progenitors led to major increased collagen deposition in OvaWAT (Figure 5J), and we observed a significant phenotypic switch in progenitors, substantiated by increased frequency of PDGFRα^{+} CD9^{high} over PDGFRα^{+} CD9^{low} progenitors in *PdgfraKI* mice (Figure 5K). Such a phenotypic switch was equally observed in the IngWAT of *PdgfraKI* mice (79.4% ± 5.5% and 97.7% ± 0.4% of PDGFRα^{+}CD9^{high} in the IngWAT from control and *PdgfraKI* HFD-fed mice, respectively, $p < 0.05$).

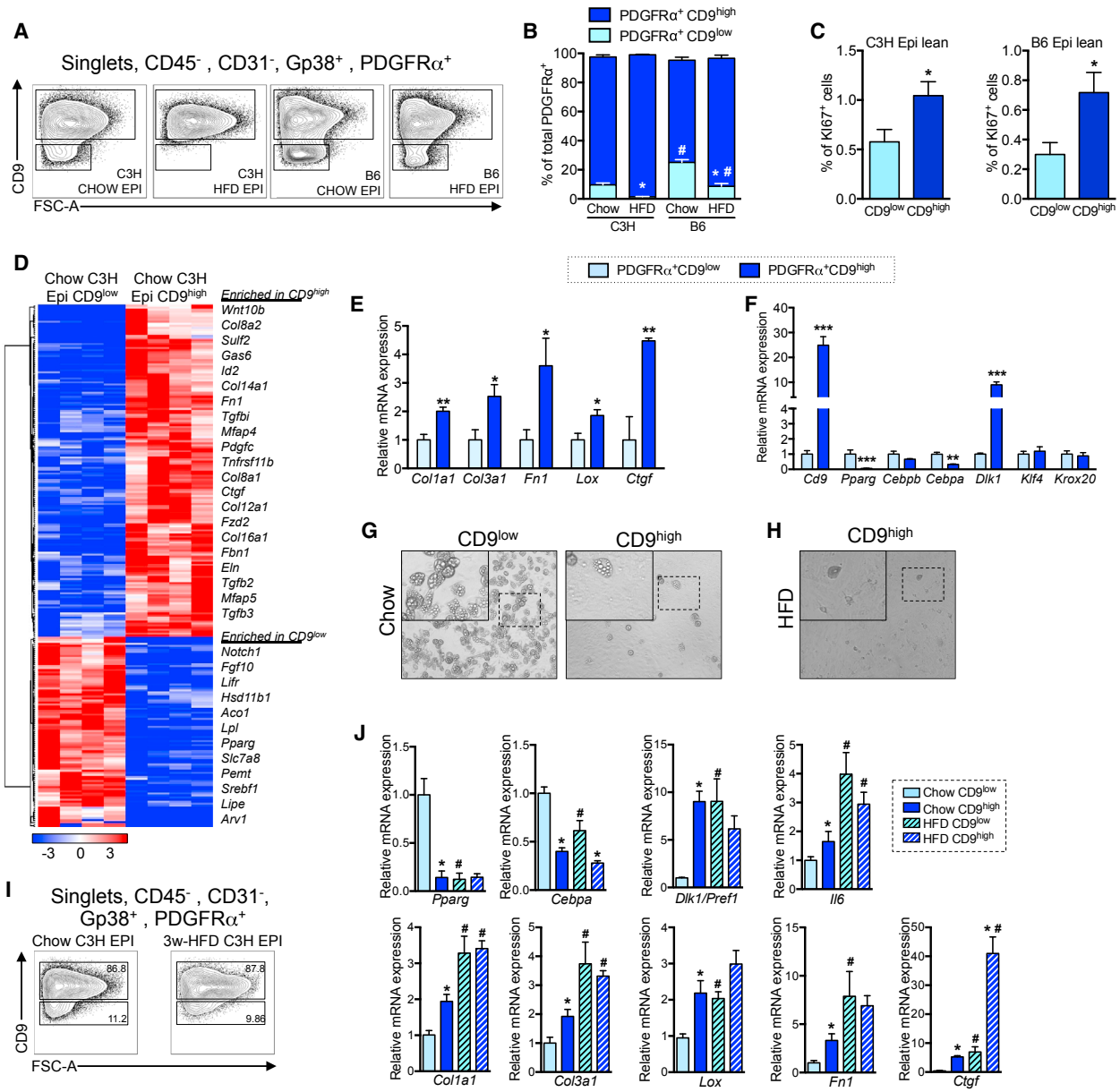

Figure 4. CD9 Expression on WAT Progenitors Identifies Pro-adipogenic and Pro-fibrotic Cell Subsets

(A–H) C3H and B6 obese mice were fed on HFD for 2 and 3 months, respectively.

(A) Flow cytograms showing expression of CD9 on CD45$^-$ CD31$^-$ Gp38$^+$ PDGFRα$^+$ progenitors in EpiWAT of chow and HFD C3H and B6 mice.

(B) Quantification of PDGFRα$^+$ CD9^{low} and PDGFRα$^+$ CD9^{high} progenitors in EpiWAT of chow and HFD C3H and B6 mice (n = 4–5).

(C) Percentage of Ki-67$^+$ cells in the PDGFRα$^+$ CD9^{low} or in the PDGFRα$^+$ CD9^{high} progenitor subsets (n = 4–5).

(D) Heatmap from hierarchical clustering of differentially expressed genes (fold change 1.5, q value < 5%) between the CD9^{low} and the CD9^{high} progenitor subsets from EpiWAT of lean C3H animals (n = 4). Red-blue color scale is used; red indicates high expression and blue indicates low expression.

(E) Relative mRNA expression measured in PDGFRα$^+$ CD9^{high} and PDGFRα$^+$ CD9^{low} cells isolated from EpiWAT of lean C3H mice (n = 4).

(F) Relative mRNA expression measured in PDGFRα$^+$ CD9^{high} and PDGFRα$^+$ CD9^{low} cells isolated from EpiWAT of lean C3H mice (n = 4); *p < 0.05, **p < 0.005, ***p < 0.0005.; *p < 0.05, **p < 0.005, ***p < 0.0005.

(G and H) Contrast phase pictures of adipocytes on day 10 post-differentiation induction in PDGFRα$^+$ CD9^{high} and PDGFRα$^+$ CD9^{low} cells isolated from EpiWAT of (G) lean and (H) obese 2 month HFD-fed C3H mice.

(I) Flow cytogram showing expression of CD9 on PDGFRα$^+$ progenitors in EpiWAT of chow and 3 week HFD-fed C3H mice.

(J) Relative mRNA expression of adipogenic or fibrotic genes measured in PDGFRα$^+$ CD9^{high} and PDGFRα$^+$ CD9^{low} cells isolated from EpiWAT of lean and 3 week HFD-fed C3H mice (n = 4–5). *p < 0.05 between CD9^{low} versus CD9^{high} progenitors in lean or obese condition; #p < 0.05 for CD9^{low} or CD9^{high} progenitors in lean versus obese condition.

Data are expressed as mean ± SEM.

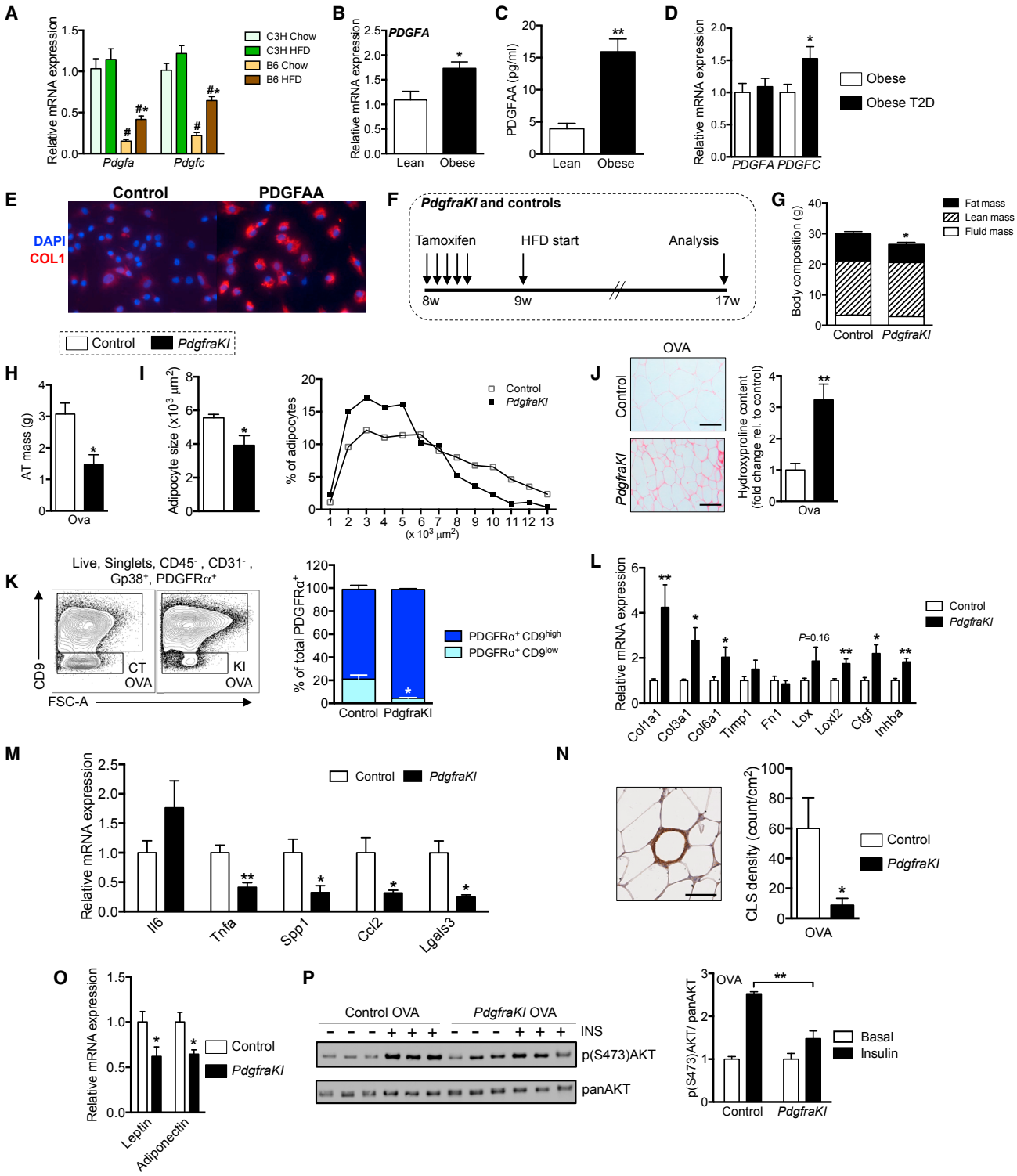

Figure 5. PDGF-PDGFRα Signaling Components in WAT Homeostasis

(A) *Pdgfa* and *Pdgfc* mRNA expression in EpiWAT of chow and HFD C3H and B6 mice (n = 5–7).

(B) *PDGFA* mRNA expression in lean (n = 7) and obese (n = 17) scWAT.

(C) Dosage of PDGFAA in conditioned medium from scWAT explants from lean (n = 7) and obese (n = 15) individuals.

(D) *PDGFA* and *PDGFC* mRNA expression in obese (n = 10) and obese with type 2 diabetes (T2D) (n = 13) oWAT.

(E) IF detection of collagen 1 (red) and DAPI (blue) in immunoselected progenitors from scWAT of lean subjects treated for 5 days with 10 ng/mL PDGFAA.

(F) Experimental design for *PdgfraKI* and control mice analysis.

(legend continued on next page)

We then further analyzed gene expression in OvaWAT and confirmed that several genes encoding for ECM components, pro-fibrotic cytokines (*Ctgf* and *Inha*), or crosslinking enzymes were upregulated in mutant animals (Figure 5L). Interestingly, most of the pro-inflammatory markers (*Tnfα*, *Ccl2*, *Spp1*, and *Lgals3*) were found to be significantly decreased (Figure 5M). Accordingly, a decreased number of crown-like structures was measured in OvaWAT of *PdgfraKI* mice (Figure 5N). Thus, the consequences of PDGFRα activation on OvaWAT phenotype could be dissociated from chronic inflammatory processes. Regarding adipokines, decreased expression of *Leptin* and *Adiponectin* mRNA was observed in the OvaWAT of *PdgfraKI* mice (Figure 5O), suggesting altered production. Insulin sensitivity in OvaWAT, measured by insulin-dependent ^{pS473}AKT induction, was reduced in *PdgfraKI* OvaWAT as compared to control littermates (Figure 5P). Altogether, the phenotypic switch toward pro-fibrotic PDGFRα$^+$ CD9^{high} progenitors observed upon PDGFRα activation contributes to the development of OvaWAT fibrosis as well as local insulin resistance in the absence of a chronic pro-inflammatory state.

Increased CD9^{high} Progenitor Pool in oWAT Correlates with Fibrosis and Metabolic Dysfunction in Obese Subjects

We then assessed whether our findings in mice could be translated to human obesity. The quantification of hydroxyproline content showed oWAT fibrosis was significantly more pronounced in patients with T2D (Figure 6A) while *COL1A1*, *COL3A1*, and *COL6A1* gene expression was unchanged in this patient subset (Figure 6B), as recently reported (Guglielmi et al., 2015). The increase in hydroxyproline content, in spite of unchanged mRNA expression of key structural collagens, suggests that mechanisms involving enhanced stabilization of collagen rather than production favor fibrotic material deposition in the oWAT (Guglielmi et al., 2015; Liu et al., 2016; Tam et al., 2012).

The phenotype of oWAT progenitor was analyzed in relation to the patients' underlying metabolic condition and the extent of oWAT fibrosis. Two progenitor populations could be distinguished in oWAT of morbidly obese individuals based on CD9 expression (Figure 6C). Mirroring the findings observed in HFD-fed C3H mice, an increased frequency of PDGFRα$^+$ CD9^{high} over PDGFRα$^+$ CD9^{low} progenitors was observed in obese subjects with glucose intolerance or diabetes (Figures 6C and 6D). A positive correlation between CD9^{high} precursor frequencies in oWAT and blood fasting glucose, fasting insulinemia, HbA1c, and the HOMA-IR index of insulin resistance was identified in obese patients (Figure 6E). Finally, PDGFRα$^+$ CD9^{high} progenitor frequencies strongly correlated with oWAT hydroxyproline content (Figure 6F).

To further gain insight into the functional differences between CD9^{high} and CD9^{low} progenitors in humans, we performed transcriptomic profiling of sorted progenitor populations isolated from oWAT of obese individuals. We investigated seven women with morbid obesity and without diabetes or glucose intolerance. Among the genes enriched in CD9^{high} precursors, we identified several chemokines (*CCL2*, *CXCL6*, and *CXCL16*), pro-inflammatory cytokines (*MIF* and *IL8*), and *LGALS3* involved in inflammation and fibrosis (Jeftic et al., 2015) (Figure 6G), suggesting CD9^{high} progenitors may affect leucocyte chemotaxis and oWAT inflammatory status. Reminiscent of the results obtained in EpiWAT after a short HFD exposure (Figure 4J), gene expression analysis in CD9^{high} and CD9^{low} precursors isolated from obese oWAT did not reveal any mRNA expression differences in ECM components such as *COL1A1*, *COL6A1*, *COL6A2*, *COL6A3*, and *COL3A1* as well as cross-linking enzymes *LOX*, *LOXL1*, *LOXL3*, and *LOXL4*. However, in these obese individuals, CD9^{low} progenitors were enriched in expression of genes related to adipogenesis (Table S2; Figure 6G), as observed in mice (Figure 4). These genes include the critical pro-adipogenic transcription factors *PPARG*, *LMO3*, *EBF1*, and *PEG10* (Jimenez et al., 2007; Lindroos et al., 2013; Hishida et al., 2007).

Together, our results suggest that an imbalance between CD9^{high} versus CD9^{low} progenitors in the oWAT of obese individuals stimulates WAT inflammation and fibrosis, predisposing toward insulin resistance and T2D.

DISCUSSION

Our work has unveiled new insights about the cellular effectors causing WAT fibrosis, which may represent a maladaptive mechanism contributing to obesity-related loss of metabolic fitness associated with many comorbidities. On the strength of ex vivo and in vivo experiments in both mouse models and human conditions, we provide new evidence that PDGFRα$^+$CD9^{high} cells within the adipogenic niche are pro-fibrosis promoting. In addition, increased numbers of PDGFRα$^+$CD9^{high} cells compared to PDGFRα$^+$CD9^{low} progenitors participate in visceral WAT fibrosis and are associated with insulin resistance and T2D. This finding adds another function to adipocyte precursors

(G and H) Body composition (G) and peri-ovarian fat (OvaWAT) mass (H) in 2 month HFD-fed control and *PdgfraKI* mice (n = 6–7).
(I) Quantification of mean adipocyte area and adipocyte size distribution in OvaWAT from control and *PdgfraKI* mice (n = 6–7).
(J) Left: representative red picrosirius-stained paraffin section of OvaWAT from HFD controls and *PdgfraKI* mutants. Right: hydroxyproline content determined in OvaWAT of HFD-fed control and *PdgfraKI* mice (n = 6–7).
(K) FACS plot showing expression of CD9 expression on CD45$^-$ CD31$^-$ Gp38$^+$ PDGFRα$^+$ progenitors in OvaWAT of HFD-fed *PdgfraKI* and control mice. Percentage of CD9^{high} and CD9^{low} PDGFRα$^+$ progenitors (n = 5).
(L) Relative mRNA expression measured in OvaWAT of HFD-fed control and *PdgfraKI* mice (n = 6).
(M) Relative mRNA expression measured in OvaWAT of HFD-fed control and *PdgfraKI* mice (n = 6).
(N) Left: representative light microscopic image of crown-like structure (CLS) in OvaWAT paraffin section stained with F4/80. Right: density of CLS in OvaWAT of control and *PdgfraKI* mice (n = 6).
(O) Relative mRNA expression of *Leptin* and *Adiponectin* in OvaWAT of control and *PdgfraKI* mice (n = 6–7).
(P) Ser473 phosphorylation of AKT (p(S473)AKT) and pan AKT expression in OvaWAT of HFD-fed control and *PdgfraKI* mice injected with insulin (+INS) or not (−INS). Quantification of p(S473)AKT normalized against panAKT relative to basal condition is presented (n = 3–4). *p < 0.05, **p < 0.005.
Data are expressed as mean ± SEM.

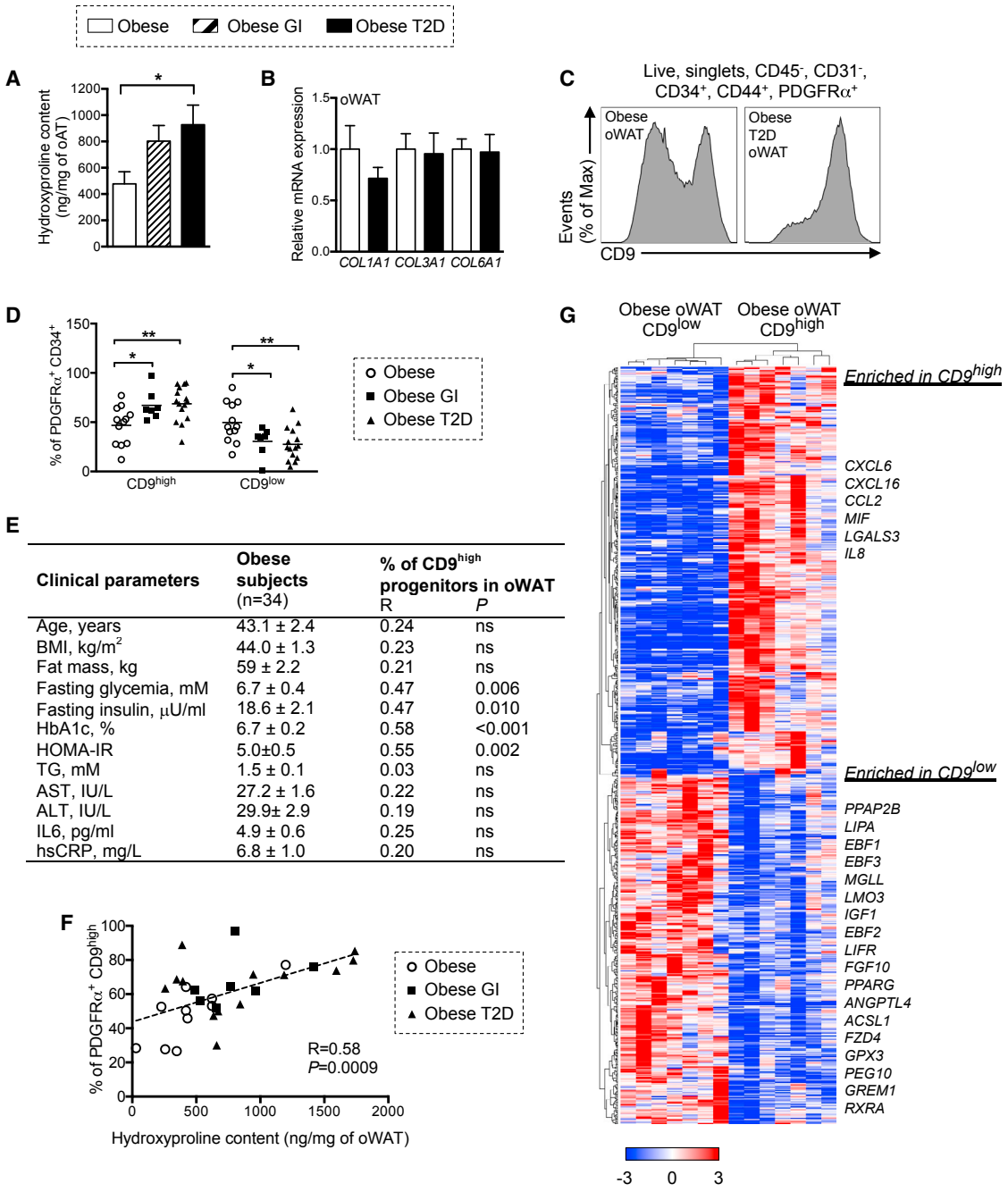

Clinical parameters	Obese subjects (n=34)	% of CD9^{high} progenitors in oWAT	
		R	*P*
Age, years	43.1 ± 2.4	0.24	ns
BMI, kg/m^2	44.0 ± 1.3	0.23	ns
Fat mass, kg	59 ± 2.2	0.21	ns
Fasting glycemia, mM	6.7 ± 0.4	0.47	0.006
Fasting insulin, μU/ml	18.6 ± 2.1	0.47	0.010
HbA1c, %	6.7 ± 0.2	0.58	<0.001
HOMA-IR	5.0±0.5	0.55	0.002
TG, mM	1.5 ± 0.1	0.03	ns
AST, IU/L	27.2 ± 1.6	0.22	ns
ALT, IU/L	29.9± 2.9	0.19	ns
IL6, pg/ml	4.9 ± 0.6	0.25	ns
hsCRP, mg/L	6.8 ± 1.0	0.20	ns

Figure 6. CD9^{high} and CD9^{low} Progenitor Subsets in oWAT of Obese Subjects

(A) Hydroxyproline content in oWAT biopsies from obese subjects with glucose intolerance (GI) (n = 7), with type 2 diabetes (T2D) (n = 13), or without GI and T2D (obese) (n = 10).

(B) *COL1A1*, *COL3A1*, and *COL6A1* mRNA expression in oWAT of obese individuals with T2D (n = 13) or without T2D (n = 10).

(C) FACS plot histogram showing CD9 expression on CD45$^-$ CD31$^-$ CD34$^+$ CD44$^+$ PDGFRα$^+$ progenitors of human oWAT from obese and obese diabetic individuals.

(D) Percentage of CD9^{high} and CD9^{low} progenitors in oWAT obtained from BMI-matched subjects with morbid obesity (n = 12), with obesity and glucose intolerance (GI) (n = 7), or with obesity and type 2 diabetes (T2D) (n = 15).

(E) Correlation analysis between percentage of CD9^{high} progenitors measured in oWAT and clinical characteristics in 34 obese patients including individuals with glucose intolerance (GI), with type 2 diabetes (T2D), or without GI and T2D. Insulin-treated patients (n = 4) were excluded from the correlation analysis with insulinemia and HOMA-IR index. Spearman's rank correlation coefficient (R) is presented.

(F) Correlation curve between hydroxyproline content and the percentage of CD9^{high} progenitors (CD45$^-$ CD31$^-$ CD34$^+$ CD44$^+$ PDGFRα$^+$ CD9^{high}) in oWAT from subjects with morbid obesity (Obese), with obesity and glucose intolerance (Obese GI), or with obesity and type 2 diabetes (Obese T2D).

(legend continued on next page)

previously implicated in cold- or β3-adrenergic-stimulated adipose beiging (Lee et al., 2012, 2013; McDonald et al., 2015), as well as developmental (Hudak et al., 2014), homeostatic (Gupta et al., 2012), and obesogenic (Jeffery et al., 2015, 2016; Vishvanath et al., 2016) white adipogenesis.

Current models of obesity, such as HFD-fed C57BL6/J (B6) mice, develop very little WAT fibrosis, which is then difficult to compare to human obese WAT. In obese C3H/HeOuj (C3H) mice that are more prone to WAT fibrosis than B6 mice (Vila et al., 2014), we showed that perigonadal WAT fibrosis was associated with lower fat accretion and higher local insulin resistance compared to obese-matched B6 mice. In these fibrosis-prone C3H obese mice, PDGFRα$^+$ progenitors were an important source of ECM production. More specifically, CD9^{high} PDGFRα$^+$ progenitors were a source of both fibrotic material and pro-inflammatory factors, arguing that CD9^{high} progenitors have a critical role in WAT remodeling and biological perturbation during obesity. In contrast, PDGFRα$^+$CD9^{low} progenitors, mostly post-mitotic, were transcriptionally committed to adipogenesis. Importantly, PDGFRα$^+$CD9^{low} progenitors rapidly became dysfunctional following the initiation of HFD, and fibrosis onset led to their almost complete disappearance. Thus, WAT fibrosis affects progenitor adipogenic capacity and may explain, at least in part, limited fat accumulation following ECM deposition.

PDGFRα signaling was instrumental in the activation of PDGFRα$^+$ progenitors toward profibrotic cells, correlating with previous studies in dermal AT (Olson and Soriano, 2009; Iwayama et al., 2015). Indeed, boosting PDGFRα signaling in a fraction of PDGFRα$^+$ progenitors favored the accumulation of CD9^{high} over CD9^{low} cells. Such a phenotypic switch was concomitant with collagen deposition and local insulin resistance. As a consequence, our observations support that PDGFRα signaling may contribute to mechanisms leading to maladaptive WAT fibrosis in obese conditions.

Important similarities were identified between humans and mice in our study. First, CD9^{high} and CD9^{low}PDGFRα$^+$ progenitors could also be detected in human oWAT obtained from severely obese subjects. Second, the frequency of PDGFRα$^+$CD9^{high} cells in oWAT of obese subjects was positively correlated with the degree of fibrosis in oWAT. Third, we reveal for the first time significant association between CD9^{high} progenitor accumulation and insulin resistance. Indeed, obese patients with the highest metabolic deterioration also had the highest number of CD9^{high} cells. Additionally, and as observed in mice, gene profiling performed on CD9^{high} and CD9^{low} human progenitors isolated from oWAT revealed CD9^{low} progenitors exhibited a pro-adipogenic molecular signature, suggesting these cells were committed to the adipogenic lineage. Similar to mice, glucose intolerant and diabetic obese individuals tended to lose CD9^{low} progenitors in WAT. Thus, obese WAT may create a local environment suitable for the phenotypic switch of adipose progenitors toward fibrogenic myofibroblasts altering WAT plasticity and precipitating the loss of metabolic fitness.

Here, we showed PDGFAA expression and secretion were upregulated in obese AT, and PDGFAA was found to stimulate collagen synthesis. Thus, PDGFAA, together with TGFβ, which is enhanced in obese AT (Fain et al., 2005; Alessi et al., 2000), may act synergistically to promote WAT fibrosis. Indeed, previous work in scleroderma showed that TGFβ was able to enhance PDGF-stimulated signaling by increasing the expression of PDGFRα (Yamakage et al., 1992). Overall, TGFβ and PDGFAA may contribute to the induction of ECM gene expression in the fibrotic AT of obese individuals.

Fibrosis is often induced in conditions of chronic inflammation (Vila et al., 2014; Wynn and Ramalingam, 2012), but it remains unknown whether fibrosis could impact local WAT inflammation. In *PdgfraKI* mutants, we observe a peculiar condition in which fibrosis induced by PDGFRα activation was not associated with WAT inflammation. Thus, while inflammation is frequently a major driver of fibrosis, the corollary is not true in *PdgfraKI* mice.

Collectively, our data reveal the central role played by PDGFRα$^+$ progenitor cell types in obesity-induced WAT fibrosis as well as their potential impact on local and systemic metabolic deterioration in humans. As a consequence, our findings raise questions about targeting WAT progenitors and developing new therapeutics to break the deleterious link between obesity and its associated metabolic dysfunction.

EXPERIMENTAL PROCEDURES

FACS Analysis

Stromal vascular fractions (SVFs) from WAT were resuspended in PBS containing 1% BSA and 0.5 mM EDTA. For mouse WAT progenitors, we used anti-PDGFRα-APC (APA5), anti-CD45-APC-eF780 (30F11), anti-CD31-PE-Cy7 (390), anti-GP38-PE (ebio8.1.1), anti-CD9-FITC (ebioSN4), anti-Ki-67-A700 (B56), anti-Sca1-PE-Cy7 (D7), anti-CD34-BV421 (MEC14.7), or anti-CD45-PE-Cy7 (30-F11) with anti-CD24-APC-eF780 (M1/69), or CD45-BV510 (30-F11) with CD31-BV510 (MEC13.3) for SVF from mT/mG reporter mice. For the sorting of macrophages, we used anti-CD45-APC-eF780, anti-F4/80-PE-Cy7 (BM8), and CD11b-APC (M1/70). Fluorescence-activated cell sorting (FACS) analysis of human AT was performed with anti-CD45-APC-eVio770 (5B1 or H130), anti-CD31-eF450 (WM59), anti-CD34-BV510 (581), anti-CD44-PE (IM7), anti-PDGFRα-AF647 (aR1), or anti-CD9-FITC (ebioSN4). FACS analysis was performed with LSRFortessa Analyzer (BD Biosciences) and cell sorting with Moflo Astrios EQ (Beckman Coulter).

Human Subjects

oWAT samples were obtained from 34 morbidly obese subjects who met the recruitment criteria for bariatric surgery (BS) (Liu et al., 2016). They were prospectively enrolled at the Institute of Cardiometabolism and Nutrition (ICAN), Department of Nutrition, and operated in the Department of Surgery, Pitié-Salpêtrière Hospital. The clinical characteristics of these subjects are described in Table S1. They were part of a clinical protocol dedicated to the study of WAT fibrosis (FibroTA program NCT01655017). Before BS, height and weight were measured by standard procedures. Blood samples were collected after a 12 hr overnight fast and clinical variables were measured as described (Liu et al., 2016). Insulin resistance was estimated by calculating HOMA-IR as (glucose [nmol/L] * insulin [μU/mL]/22.5) using fasting values (Matthews et al., 1985). HOMA-IR was not calculated for insulin-treated patients. Glucose intolerance and T2D were diagnosed in accordance with ADA definition (American Diabetes Association, 2015). Obese

(G) Heatmap from hierarchical clustering of differentially expressed genes between the CD9^{low} and the CD9^{high} progenitor subsets from oWAT of obese women (n = 7); fold change > 1.5 and q value < 5%. Red-blue color scale is used; red indicates high expression and blue indicates low expression. *p < 0.05, **p < 0.005.

Data are expressed as mean ± SEM.

subjects involved for the data presented in Figures 5B and 5C were previously described (Liu et al., 2016). Ethical approval was obtained from the Research Ethics Committee of Hôtel-Dieu Hospital (Comité de Protection des Personnes, Ile de France). Informed written consent was obtained from all subjects.

Collagen Content

Hydroxyproline measurement (Khan et al., 2009) was done using a hydroxyproline colorimetric assay (BioVision). Briefly, frozen fat is weighted and heated in 6 N HCl at 110°C overnight in sealed tubes, as 10 μL of HCl/mg of WAT. Ten microliters are evaporated before incubation with chloramine-T and *p*-dimethyl-amino-benzaldehyde (DMAB) at 60°C for 90 min. The absorbance was read at 560 nm and the concentration was determined using the standard curve created with hydroxyproline.

In Vitro Adipogenesis

$CD9^{high}$ and $CD9^{low}$ progenitor subsets were sorted and seeded at high density (125.10^4 cells/cm^2) in Lab-Tek 16-well glass slide (Thermo Fisher Scientific). Cells were cultured in DMEM supplemented 10% FBS, then adipogenesis was induced with DMEM 10% FBS, 0.25 μg/mL dexamethasone, 0.5 mM isobutylmethylxanthine, and 1 μg/mL insulin for 48 hr and DMEM 10% FBS containing insulin for 48 hr and maintained in DMEM 10% FBS until day 10 post-adipogenesis induction (Marcelin et al., 2013).

Statistical Analysis

Data are expressed as mean ± SEM. One-way ANOVA was used to compare more than two groups and Holm-Sidak's parametric multiple comparisons for post hoc analysis; a Student's t test was used to compare two groups. For small sample size (i.e., $n < 30$), data were first transformed by natural logarithm if they did not follow a Gaussian distribution. Correlations were examined with non-parametric Spearman correlation test. All analyses were conducted using R software (http://www.r-project.org) and GraphPad Prism. Significance is accepted at $p < 0.05$.

ACCESSION NUMBERS

The accession number for the microarray data of $CD9^{high}$ and $CD9^{low}$ progenitors isolated from adipose tissue reported in this paper is GEO: GSE84823.

SUPPLEMENTAL INFORMATION

Supplemental Information includes Supplemental Experimental Procedures, five figures, and two tables and can be found with this article online at http://dx.doi.org/10.1016/j.cmet.2017.01.010.

AUTHOR CONTRIBUTIONS

G.M. designed, performed, analyzed, and interpreted experiments and wrote the manuscript. A.F., Y.L., V.P., Y.B., M. Ambrosini, M.F., and C.R. performed and analyzed data. M. Atlan, J.A.-W., C.P., A.T., R.N.-B., and J.-C.B. supervised enrollment and clinical phenotyping of obese subjects. C.H. performed data analysis. J.-S.H. provided the mutant mice. E.L.G. designed, analyzed, and interpreted experiments and wrote the manuscript. K.C. performed data interpretation, guidance, and manuscript writing. All authors critically read the manuscript.

ACKNOWLEDGMENTS

We thank the Institute of Cardiometabolism and Nutrition Core Facility PreclinICAN mouse phenotyping core (Amelie Lacombe and Thierry Huby). We thank Nicolas Philibert and Sonia Mutel for their technical help and Sophie Nadaud for sharing the PDGFRα-CreERT2 and *PDGFRα*$^{+/D842V}$ mouse lines. We acknowledge Rachel Peat for her critical editing of the manuscript. The clinical work was partly supported by clinical research contracts (FibroTA to J.A.-W. and K.C.). Funding was obtained from the Fondation pour la Recherche Médicale (DEQ20120323701), the French National Agency of Research (ANR), Adipofib program, the national program "Investissement d'Avenir" ANR-10-IAHU-05, and as part of the second "Investissements d'Avenir" Carmma program ANR-15-RHUS-0003. E.L.G. was supported by ANR Lipocamd program ANR-14-CE12-0017-03, ANR Maclear program ANR-15-CE14-0015-02, and the Fondation de France (00056835). A.F. was supported by Coordenação de Aperfeiçoamento de Pessoal de Nível Superior (CAPES). We thank patients and nurses, as well as Valentine Lemoine and Dr Marchelli for patient recruitment and data management aspects.

Received: August 24, 2016
Revised: November 24, 2016
Accepted: January 19, 2017
Published: February 16, 2017

REFERENCES

Alessi, M.C., Bastelica, D., Morange, P., Berthet, B., Leduc, I., Verdier, M., Geel, O., and Juhan-Vague, I. (2000). Plasminogen activator inhibitor 1, transforming growth factor-beta1, and BMI are closely associated in human adipose tissue during morbid obesity. Diabetes *49*, 1374–1380.

American Diabetes Association (2015). (2) Classification and diagnosis of diabetes. Diabetes Care *38* (*Suppl*), S8–S16.

Chun, T.H., Hotary, K.B., Sabeh, F., Saltiel, A.R., Allen, E.D., and Weiss, S.J. (2006). A pericellular collagenase directs the 3-dimensional development of white adipose tissue. Cell *125*, 577–591.

Cuylen, S., Blaukopf, C., Politi, A.Z., Müller-Reichert, T., Neumann, B., Poser, I., Ellenberg, J., Hyman, A.A., and Gerlich, D.W. (2016). Ki-67 acts as a biological surfactant to disperse mitotic chromosomes. Nature *535*, 308–312.

Dalmas, E., Venteclef, N., Caer, C., Poitou, C., Cremer, I., Aron-Wisnewsky, J., Lacroix-Desmazes, S., Bayry, J., Kaveri, S.V., Clément, K., et al. (2014). T cell-derived IL-22 amplifies IL-1β-driven inflammation in human adipose tissue: relevance to obesity and type 2 diabetes. Diabetes *63*, 1966–1977.

Divoux, A., Tordjman, J., Lacasa, D., Veyrie, N., Hugol, D., Aissat, A., Basdevant, A., Guerre-Millo, M., Poitou, C., Zucker, J.D., et al. (2010). Fibrosis in human adipose tissue: composition, distribution, and link with lipid metabolism and fat mass loss. Diabetes *59*, 2817–2825.

Estève, D., Boulet, N., Volat, F., Zakaroff-Girard, A., Ledoux, S., Coupaye, M., Decaunes, P., Belles, C., Gaits-Iacovoni, F., Iacovoni, J.S., et al. (2015). Human white and brite adipogenesis is supported by MSCA1 and is impaired by immune cells. Stem Cells *33*, 1277–1291.

Fain, J.N., Tichansky, D.S., and Madan, A.K. (2005). Transforming growth factor beta1 release by human adipose tissue is enhanced in obesity. Metabolism *54*, 1546–1551.

Guglielmi, V., Cardellini, M., Cinti, F., Corgosinho, F., Cardolini, I., D'Adamo, M., Zingaretti, M.C., Bellia, A., Lauro, D., Gentileschi, P., et al. (2015). Omental adipose tissue fibrosis and insulin resistance in severe obesity. Nutr. Diabetes *5*, e175.

Gupta, R.K., Mepani, R.J., Kleiner, S., Lo, J.C., Khandekar, M.J., Cohen, P., Frontini, A., Bhowmick, D.C., Ye, L., Cinti, S., and Spiegelman, B.M. (2012). Zfp423 expression identifies committed preadipocytes and localizes to adipose endothelial and perivascular cells. Cell Metab. *15*, 230–239.

Halberg, N., Khan, T., Trujillo, M.E., Wernstedt-Asterholm, I., Attie, A.D., Sherwani, S., Wang, Z.V., Landskroner-Eiger, S., Dineen, S., Magalang, U.J., et al. (2009). Hypoxia-inducible factor 1alpha induces fibrosis and insulin resistance in white adipose tissue. Mol. Cell. Biol. *29*, 4467–4483.

Henegar, C., Tordjman, J., Achard, V., Lacasa, D., Cremer, I., Guerre-Millo, M., Poitou, C., Basdevant, A., Stich, V., Viguerie, N., et al. (2008). Adipose tissue transcriptomic signature highlights the pathological relevance of extracellular matrix in human obesity. Genome Biol. *9*, R14.

Hishida, T., Naito, K., Osada, S., Nishizuka, M., and Imagawa, M. (2007). peg10, an imprinted gene, plays a crucial role in adipocyte differentiation. FEBS Lett. *581*, 4272–4278.

Holley, R.J., Tai, G., Williamson, A.J., Taylor, S., Cain, S.A., Richardson, S.M., Merry, C.L., Whetton, A.D., Kielty, C.M., and Canfield, A.E. (2015). Comparative quantification of the surfaceome of human multipotent mesenchymal progenitor cells. Stem Cell Reports *4*, 473–488.

Hotamisligil, G.S., Shargill, N.S., and Spiegelman, B.M. (1993). Adipose expression of tumor necrosis factor-alpha: direct role in obesity-linked insulin resistance. Science *259*, 87–91.

Hudak, C.S., Gulyaeva, O., Wang, Y., Park, S.M., Lee, L., Kang, C., and Sul, H.S. (2014). Pref-1 marks very early mesenchymal precursors required for adipose tissue development and expansion. Cell Rep. *8*, 678–687.

Ibrahim, M.M. (2010). Subcutaneous and visceral adipose tissue: structural and functional differences. Obes. Rev. *11*, 11–18.

Iwayama, T., Steele, C., Yao, L., Dozmorov, M.G., Karamichos, D., Wren, J.D., and Olson, L.E. (2015). PDGFRα signaling drives adipose tissue fibrosis by targeting progenitor cell plasticity. Genes Dev. *29*, 1106–1119.

Jeffery, E., Church, C.D., Holtrup, B., Colman, L., and Rodeheffer, M.S. (2015). Rapid depot-specific activation of adipocyte precursor cells at the onset of obesity. Nat. Cell Biol. *17*, 376–385.

Jeffery, E., Wing, A., Holtrup, B., Sebo, Z., Kaplan, J.L., Saavedra-Peña, R., Church, C.D., Colman, L., Berry, R., and Rodeheffer, M.S. (2016). The adipose tissue microenvironment regulates depot-specific adipogenesis in obesity. Cell Metab. *24*, 142–150.

Jeftic, I., Jovicic, N., Pantic, J., Arsenijevic, N., Lukic, M.L., and Pejnovic, N. (2015). Galectin-3 ablation enhances liver steatosis, but attenuates inflammation and IL-33-dependent fibrosis in obesogenic mouse model of nonalcoholic steatohepatitis. Mol. Med. *21*, 453–465.

Jimenez, M.A., Akerblad, P., Sigvardsson, M., and Rosen, E.D. (2007). Critical role for Ebf1 and Ebf2 in the adipogenic transcriptional cascade. Mol. Cell. Biol. *27*, 743–757.

Joe, A.W., Yi, L., Natarajan, A., Le Grand, F., So, L., Wang, J., Rudnicki, M.A., and Rossi, F.M. (2010). Muscle injury activates resident fibro/adipogenic progenitors that facilitate myogenesis. Nat. Cell Biol. *12*, 153–163.

Khan, T., Muise, E.S., Iyengar, P., Wang, Z.V., Chandalia, M., Abate, N., Zhang, B.B., Bonaldo, P., Chua, S., and Scherer, P.E. (2009). Metabolic dysregulation and adipose tissue fibrosis: role of collagen VI. Mol. Cell. Biol. *29*, 1575–1591.

Kim, Y.J., Yu, J.M., Joo, H.J., Kim, H.K., Cho, H.H., Bae, Y.C., and Jung, J.S. (2007). Role of CD9 in proliferation and proangiogenic action of human adipose-derived mesenchymal stem cells. Pflugers Arch. *455*, 283–296.

Kissebah, A.H., and Krakower, G.R. (1994). Regional adiposity and morbidity. Physiol. Rev. *74*, 761–811.

Lee, Y.H., Petkova, A.P., Mottillo, E.P., and Granneman, J.G. (2012). In vivo identification of bipotential adipocyte progenitors recruited by β3-adrenoceptor activation and high-fat feeding. Cell Metab. *15*, 480–491.

Lee, Y.H., Petkova, A.P., and Granneman, J.G. (2013). Identification of an adipogenic niche for adipose tissue remodeling and restoration. Cell Metab. *18*, 355–367.

Lindroos, J., Husa, J., Mitterer, G., Haschemi, A., Rauscher, S., Haas, R., Gröger, M., Loewe, R., Kohrgruber, N., Schrögendorfer, K.F., et al. (2013). Human but not mouse adipogenesis is critically dependent on LMO3. Cell Metab. *18*, 62–74.

Liu, Y., Aron-Wisnewsky, J., Marcelin, G., Genser, L., Le Naour, G., Torcivia, A., Bauvois, B., Bouchet, S., Pelloux, V., Sasso, M., et al. (2016). Accumulation and changes in composition of collagens in subcutaneous adipose tissue after bariatric surgery. J. Clin. Endocrinol. Metab. *101*, 293–304.

Marcelin, G., Liu, S.M., Schwartz, G.J., and Chua, S.C., Jr. (2013). Identification of a loss-of-function mutation in Ube2l6 associated with obesity resistance. Diabetes *62*, 2784–2795.

Matthews, D.R., Hosker, J.P., Rudenski, A.S., Naylor, B.A., Treacher, D.F., and Turner, R.C. (1985). Homeostasis model assessment: insulin resistance and beta-cell function from fasting plasma glucose and insulin concentrations in man. Diabetologia *28*, 412–419.

McDonald, M.E., Li, C., Bian, H., Smith, B.D., Layne, M.D., and Farmer, S.R. (2015). Myocardin-related transcription factor A regulates conversion of progenitors to beige adipocytes. Cell *160*, 105–118.

Olson, L.E., and Soriano, P. (2009). Increased PDGFRalpha activation disrupts connective tissue development and drives systemic fibrosis. Dev. Cell *16*, 303–313.

Osborn, O., and Olefsky, J.M. (2012). The cellular and signaling networks linking the immune system and metabolism in disease. Nat. Med. *18*, 363–374.

Pasarica, M., Gowronska-Kozak, B., Burk, D., Remedios, I., Hymel, D., Gimble, J., Ravussin, E., Bray, G.A., and Smith, S.R. (2009). Adipose tissue collagen VI in obesity. J. Clin. Endocrinol. Metab. *94*, 5155–5162.

Pellegrinelli, V., Heuvingh, J., du Roure, O., Rouault, C., Devulder, A., Klein, C., Lacasa, M., Clément, E., Lacasa, D., and Clément, K. (2014a). Human adipocyte function is impacted by mechanical cues. J. Pathol. *233*, 183–195.

Rivers, L.E., Young, K.M., Rizzi, M., Jamen, F., Psachoulia, K., Wade, A., Kessaris, N., and Richardson, W.D. (2008). PDGFRA/NG2 glia generate myelinating oligodendrocytes and piriform projection neurons in adult mice. Nat. Neurosci. *11*, 1392–1401.

Rodeheffer, M.S., Birsoy, K., and Friedman, J.M. (2008). Identification of white adipocyte progenitor cells in vivo. Cell *135*, 240–249.

Spencer, M., Yao-Borengasser, A., Unal, R., Rasouli, N., Gurley, C.M., Zhu, B., Peterson, C.A., and Kern, P.A. (2010). Adipose tissue macrophages in insulin-resistant subjects are associated with collagen VI and fibrosis and demonstrate alternative activation. Am. J. Physiol. Endocrinol. Metab. *299*, E1016–E1027.

Sun, K., Kusminski, C.M., and Scherer, P.E. (2011). Adipose tissue remodeling and obesity. J. Clin. Invest. *121*, 2094–2101.

Sun, K., Tordjman, J., Clément, K., and Scherer, P.E. (2013). Fibrosis and adipose tissue dysfunction. Cell Metab. *18*, 470–477.

Tam, C.S., Tordjman, J., Divoux, A., Baur, L.A., and Clément, K. (2012). Adipose tissue remodeling in children: the link between collagen deposition and age-related adipocyte growth. J. Clin. Endocrinol. Metab. *97*, 1320–1327.

Uezumi, A., Fukada, S., Yamamoto, N., Takeda, S., and Tsuchida, K. (2010). Mesenchymal progenitors distinct from satellite cells contribute to ectopic fat cell formation in skeletal muscle. Nat. Cell Biol. *12*, 143–152.

Uezumi, A., Ito, T., Morikawa, D., Shimizu, N., Yoneda, T., Segawa, M., Yamaguchi, M., Ogawa, R., Matev, M.M., Miyagoe-Suzuki, Y., et al. (2011). Fibrosis and adipogenesis originate from a common mesenchymal progenitor in skeletal muscle. J. Cell Sci. *124*, 3654–3664.

Vila, I.K., Badin, P.M., Marques, M.A., Monbrun, L., Lefort, C., Mir, L., Louche, K., Bourlier, V., Roussel, B., Gui, P., et al. (2014). Immune cell Toll-like receptor 4 mediates the development of obesity- and endotoxemia-associated adipose tissue fibrosis. Cell Rep. *7*, 1116–1129.

Vishvanath, L., MacPherson, K.A., Hepler, C., Wang, Q.A., Shao, M., Spurgin, S.B., Wang, M.Y., Kusminski, C.M., Morley, T.S., and Gupta, R.K. (2016). Pdgfrβ+ mural preadipocytes contribute to adipocyte hyperplasia induced by high-fat-diet feeding and prolonged cold exposure in adult mice. Cell Metab. *23*, 350–359.

Wajchenberg, B.L. (2000). Subcutaneous and visceral adipose tissue: their relation to the metabolic syndrome. Endocr. Rev. *21*, 697–738.

Weisberg, S.P., McCann, D., Desai, M., Rosenbaum, M., Leibel, R.L., and Ferrante, A.W., Jr. (2003). Obesity is associated with macrophage accumulation in adipose tissue. J. Clin. Invest. *112*, 1796–1808.

Wynn, T.A. (2008). Cellular and molecular mechanisms of fibrosis. J. Pathol. *214*, 199–210.

Wynn, T.A., and Ramalingam, T.R. (2012). Mechanisms of fibrosis: therapeutic translation for fibrotic disease. Nat. Med. *18*, 1028–1040.

Yamakage, A., Kikuchi, K., Smith, E.A., LeRoy, E.C., and Trojanowska, M. (1992). Selective upregulation of platelet-derived growth factor alpha receptors by transforming growth factor beta in scleroderma fibroblasts. J. Exp. Med. *175*, 1227–1234.